Supplementary information

The following supplementary information contains: The flow, translocation time, occupancy number and radial distribution function for the PBC model without reservoirs; the flow, translocation time and occupancy number for different C-O interactions; the flow, translocation time, occupancy number and radial distribution function for the TIP4P/2005 water model; the flow, translocation time, occupancy number and for the system with water number N = 4473, 8946 and 13419; the flow, translocation time, occupancy number and radial distribution function for the rigid graphene channel (freeze carbon atoms) and flexible graphene channel (release carbon atoms).

Length-dependent water permeation through a graphene channel

Zi Wang[1], Shuang Li[1], Shiwu Gao*[,2], Jiaye Su*[,1]

[1]MIIT Key Laboratory of Semiconductor Microstructure and Quantum Sensing, and Department of Applied Physics, Nanjing University of Science and Technology, Nanjing 210094, China

[2]Beijing Computational Science Research Center, Beijing 100193, China

*Corresponding atuhor: swgao@csrc.ac.cn; jysu@njust.edu.cn

The flow, translocation time, occupancy number and radial distribution function for the PBC model without reservoirs.

In order to consider the effect of boundary condition, we construct a system with periodic boundary condition (PBC) in the x-z direction without water reserviors. As shown in Figure S1a, the two parallel graphene sheets separate the external water. The layer distance between the two graphene sheets is 0.68 nm, which accommodates a typical water monolayer. Figure S1b presents the flow as a function of the channel length L for the PBC and water box (main text) models. Obviously, the water flow of both models show a similar rapid decay, and the values are close to each other. With the increase in channel length, the structure of monolayer water undergoes significant changes and becomes a stable and ordered ice structure in both two models for $L \geq 2.5$ nm, resulting in zero flow. The translocation time for the two models show a similar increasing trend with the increase in channel length, shown in Figure S1c. The increasing channel length leads to a significant increase in the translocation time, which causes the water flow reduction. As seen in Figure S1d, the water occupancy number for the two models is completely overlapped, showing a linear relationship with the channel length. As seen in Figure S1e, for the monolayer water in the PBC model, the radial distribution functions (RDFs) for L = 1 and 1.5 nm have only one

peak, and then gradually become uniform, implying a liquid state. For $L \geq 2.5$ nm, the additional two peaks becomes obvious and the peak height increases significantly, indicating the formation of monolayer ice. These RDFs are quite similar to the water box model in the main text. Overall, the PBC model obtains similar results.

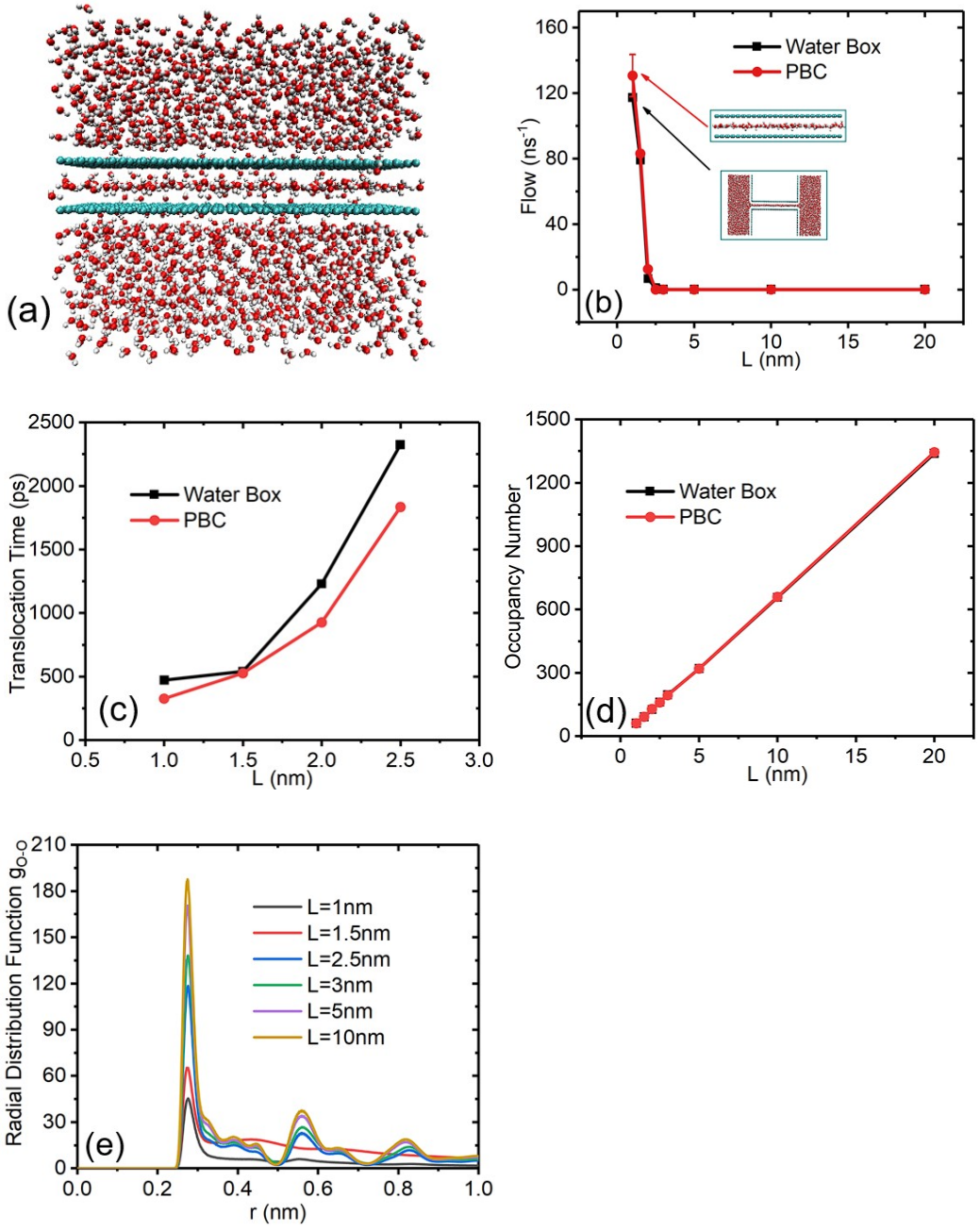

Figure S1. (a) Snapshot of the PBC simulation system without reservoirs. (b) Water flow, (c) translocation time and (d) occupancy umber as a function of the channel length. (e) Radial distribution functions of the confined water for the PBC model.

The flow, translocation time and occupancy number for different C-O interactions.

In our simulation, the carbon atoms of graphene channel are modeled by uncharged Lennard-Jones (LJ) particles in the Amber 03 force field and the water molecules are described by the simple point charge-extended (SPC/E) model, and the corresponding LJ parameters are shown in Table S1. The potential of water-carbon is $\varepsilon_{c\text{-}o}$ = 0.4836 kJ/mol. Considering that different interactions between carbon and water can have a significant impact on the water transport, we also conducted a series of simulations by modifying the C-O interaction. The simulation model remains unchanged, and the C-O interactions are set as $\varepsilon/\varepsilon_{c\text{-}o}$ = 0.7, $\varepsilon/\varepsilon_{c\text{-}o}$ = 1.0 (original parameter), $\varepsilon/\varepsilon_{c\text{-}o}$ = 1.5 and $\varepsilon/\varepsilon_{c\text{-}o}$ = 2.0, respectively. We show the water flow as a function of the channel length L in Figure S2a. For the maximum value of $\varepsilon/\varepsilon_{c\text{-}o}$ = 2.0, the water flow is almost zero even at L = 1 nm, suggesting that the water molecules are in a frozen state. However, as $\varepsilon/\varepsilon_{c\text{-}o}$ decreases, the water flow increases sharply within the range of $L \leq 2.5$ nm, which can be well explained by the competition between water-water and water-channel interactions. For $\varepsilon/\varepsilon_{c\text{-}o}$ = 0.7, owing to the significantly reduced C-O interaction, the water flow becomes quite large at small L, and ultimately becomes zero at L = 10 nm. As seen in Figure S2b, the translocation time has an opposite behavior compared to the flow, and also is sensitive to $\varepsilon/\varepsilon_{c\text{-}o}$. The occupancy numbers in Figure S2c for different $\varepsilon/\varepsilon_{c\text{-}o}$ are almost overlapped. In summary, although the water dynamics is sensitive to the $\varepsilon/\varepsilon_{c\text{-}o}$ values, the freezing phenomenon of water molecules still occurs by changing the channel length.

Table S1: Non−bonded parameters for all atom types in the main text.

Atom type	σ_i(Å)	ε_i(kJ/mol)	Charge(e)
C	3.3997	0.3598	0
O (H_2O)	3.169	0.6502	-0.8476
H (H_2O)	0	0	0.4238

The Lorentz−Bertelot rule is used to determine the parameters between different atoms, i.e., $\sigma_{ij} = (\sigma_i+\sigma_j)/2$ and $\varepsilon_{ij} = (\varepsilon_i\varepsilon_j)^{1/2}$

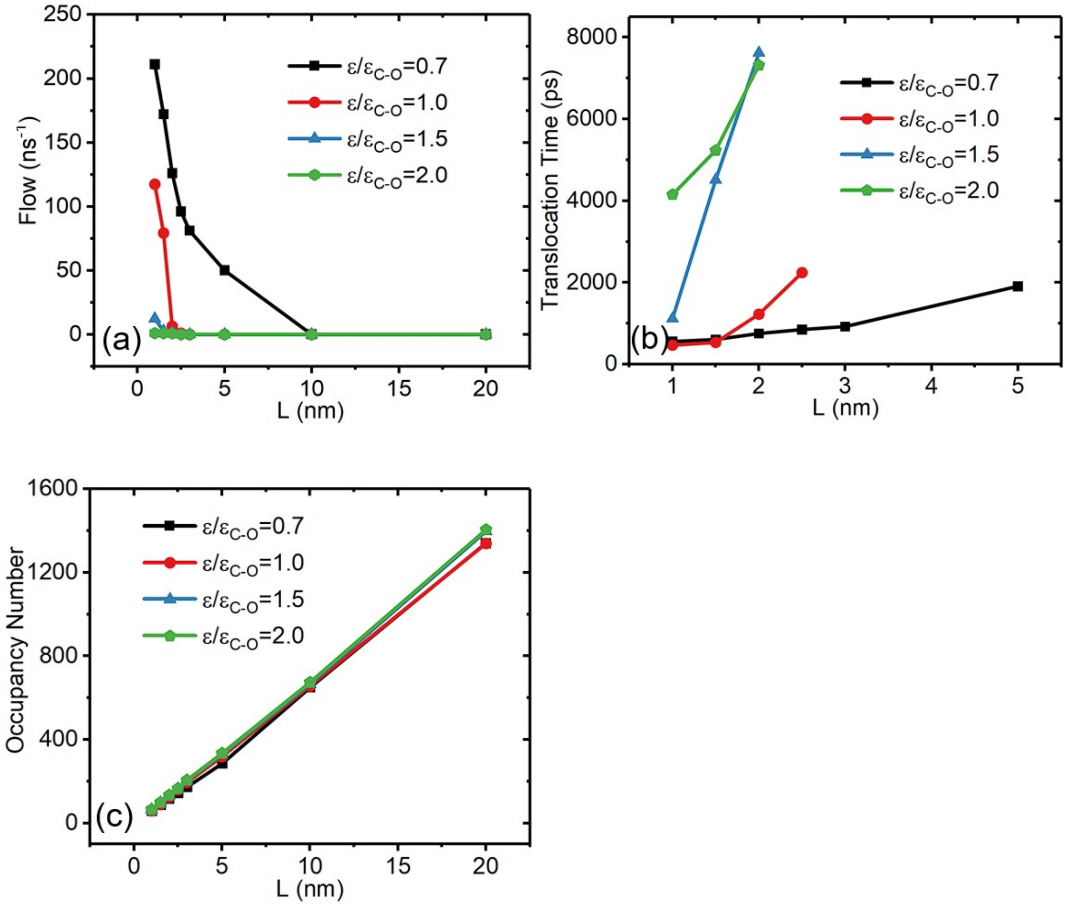

Figure S2. (a) Water flow and (b) translocation time and (c) occupancy number as a function of the channel length *L* for different C-O interactions.

The flow, translocation time, occupancy number and radial distribution function for the TIP4P/2005 water model.

Both the TIP4P/ICE and TIP4P/2005 water models have been widely used to study the properties of water. The difference is that the parameters of TIP4P/ICE model have been optimized for the characteristics of ice, which can simulate the formation and properties of ice well. Therefore, it does not match the experimental values when simulating the some relevant characteristics of liquid water [S1]. Hence we chose the TIP4P/2005 model to compare with the SPC/E model. Figure S3a displays the flow of two water models as a function of the channel length L. Both models exhibit nearly identical behavior. In short channels ($L \leq 2.5$ nm), the TIP4P/2005 model has a lower self-diffusion coefficient ($D = 2.08\times10^{-5}$ cm^2/s) and thus has a reduced water flow compared to the SPC/E model [S2]. For $L > 2.5$ nm, the two water models change to a frozen state, resulting in zero flow. Moreover, as seen in Figure S3b, the translocation time of TIP4P/2005 model has greater values because of smaller diffusion coefficients, but has a similar rising behavior with the increase in channel length. The occupancy numbers in Figure S3c both display excellent linear behaviors with a slight bifurcation due to the greater $\varepsilon_{O\text{-}O}$ (~0.776 kJ/mol) of TIP4P/2005. As seen in Figure S3d, for the monolayer water case, the RDFs for the TIP4P/2005 model is quite similar to the SPC/E model in main text, i.e., for $L \geq 2.5$ nm, the additional two peaks become obvious and the peak height increases significantly, corresponding to the ice structures. Thus, we can conclude that the main results and conclusion for the TIP4P/2005 water model should be identical to those of the SPC/E water model in this work.

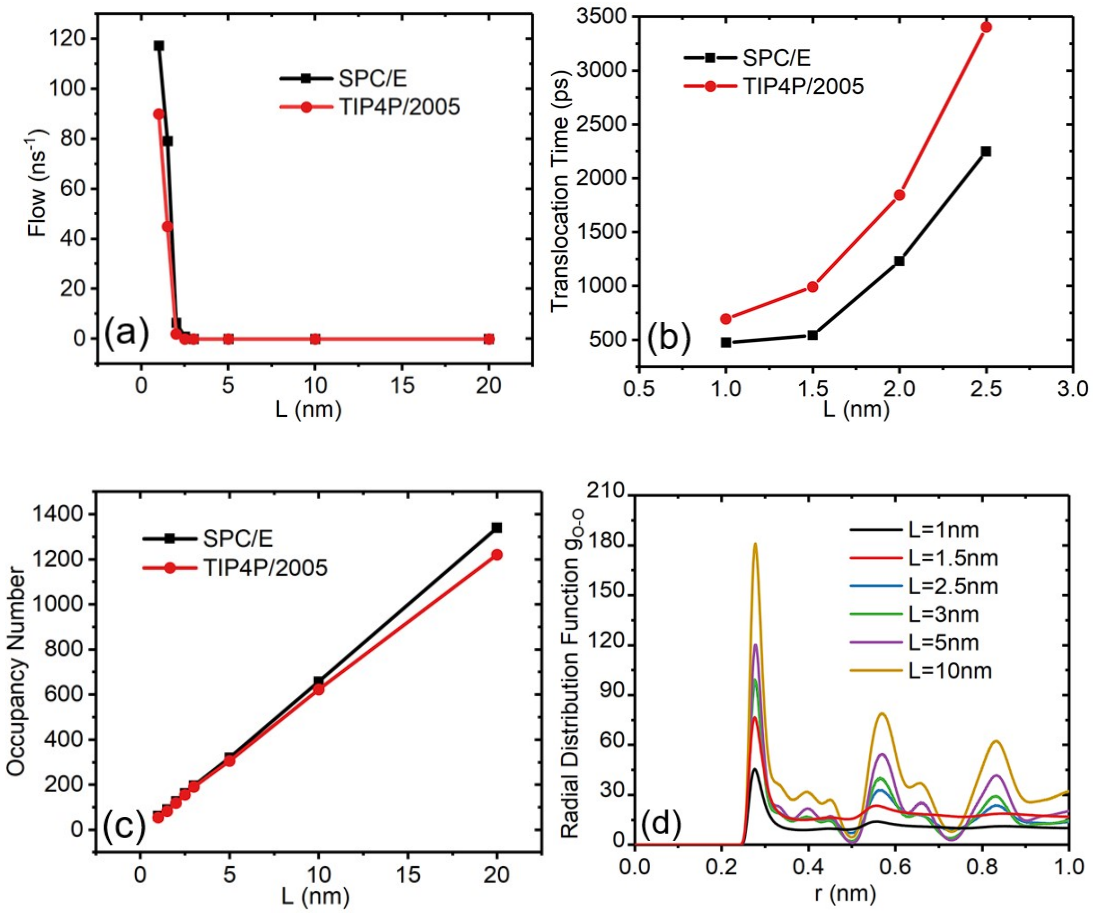

Figure S3. (a) Water flow, (b) translocation time and (c) occupancy number as a function of the channel length L for the SPC/E and TIP4P/2005 water models respectively. (d) Radial distribution functions of confined water for the TIP4P/2005 water model.

The flow, translocation time and occupancy number for the systems with total water number of N = 4473, 8946 and 13419.

To investigate the finite-size effects, we constructed additional two systems with double (N = 8946) and triple (N = 13419) water numbers. We can see from Figure S4 that the flow, translocation time and occupancy number for the three systems are almost overlapped with reasonable fluctuations. Therefore, the present system size (N = 4473) in our main text should be large enough to obtain reliable results.

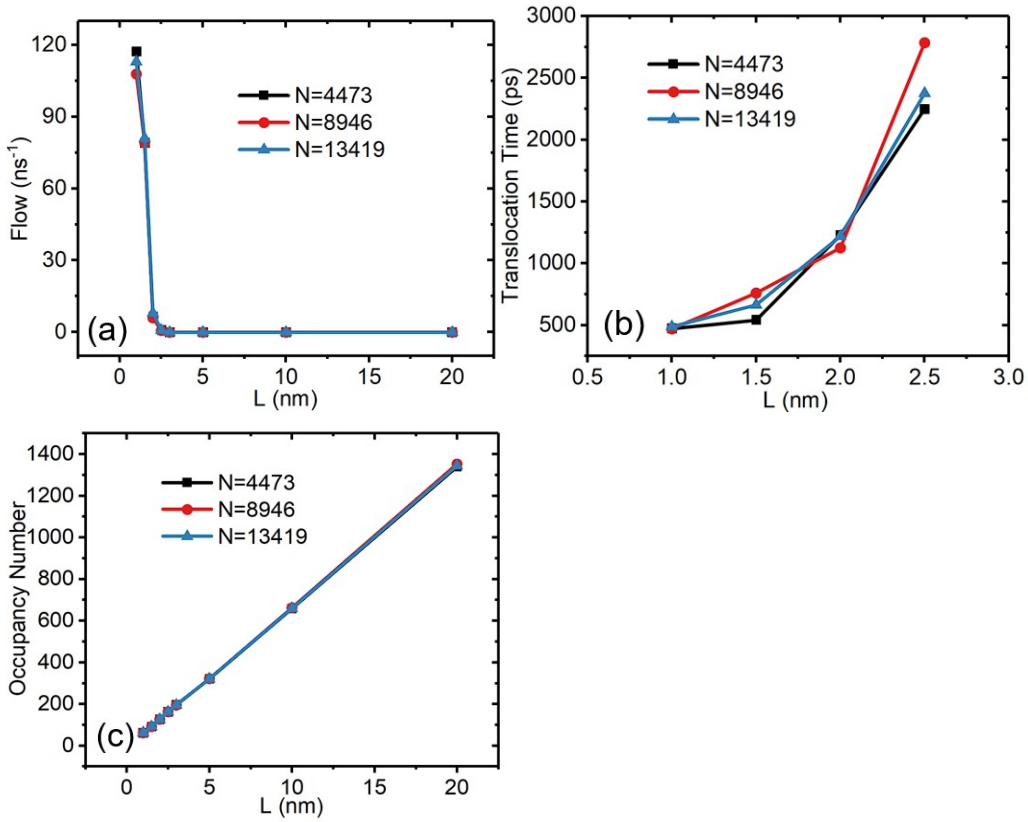

Figure S4. (a) Water flow, (b) translocation time and (c) occupancy number as a function of the channel length *L* for different water numbers *N*.

The flow, translocation time, occupancy number and radial distribution function for the rigid graphene channel (freeze carbon atoms) and flexible graphene channel (release carbon atoms).

In order to assess the effect of frozen graphene channels in the simulation, we performed additional MD simulations for the flexible graphene model. To keep the overall position of channel, we imposed positional constraints on the carbon atoms at the channel inlet and outlet. As shown in Figure S5a, the two parallel flexible graphene sheets separate the external water. The layer distance between the two graphene sheets is 0.68 nm, which accommodates a typical water monolayer. Figure S5b presents the flow as a function of the channel length *L* for the rigid and flexible graphene channels. Obviously, the water flow of both models shows a similar rapid

decay with the increase in channel length, and the structure of monolayer water undergoes significant changes and becomes a stable and ordered ice structure in both two models for $L \geq 2.5$ nm, resulting in zero flow. Notably, for $L \leq 2.5$ nm, the water flow for the flexible graphene is obviously greater because of the collision between water and graphene. The translocation time for the two models show a similar increasing trend with the increase in channel length, shown in Figure S5c. The flexible graphene has smaller translocation time that corresponds to its greater flow. The increasing channel length leads to a significant increase in the translocation time, which causes the water flow reduction. As seen in Figure S5d, the water occupancy number for the two models is completely overlapped, showing a linear relationship with the channel length. As seen in Figure S5e, for the monolayer water in the flexible channel model, the radial distribution functions (RDFs) for L = 1 and 1.5 nm have only one peak, and then gradually become uniform, implying a liquid state. For $L \geq$ 2.5 nm, the additional two peaks become obvious and the peak height increases significantly, indicating the formation of monolayer ice. These RDFs are quite similar to the rigid channel model in Figure S1. Overall, the flexible graphene channel model obtains similar results, including the critical channel length of 2.5 nm.

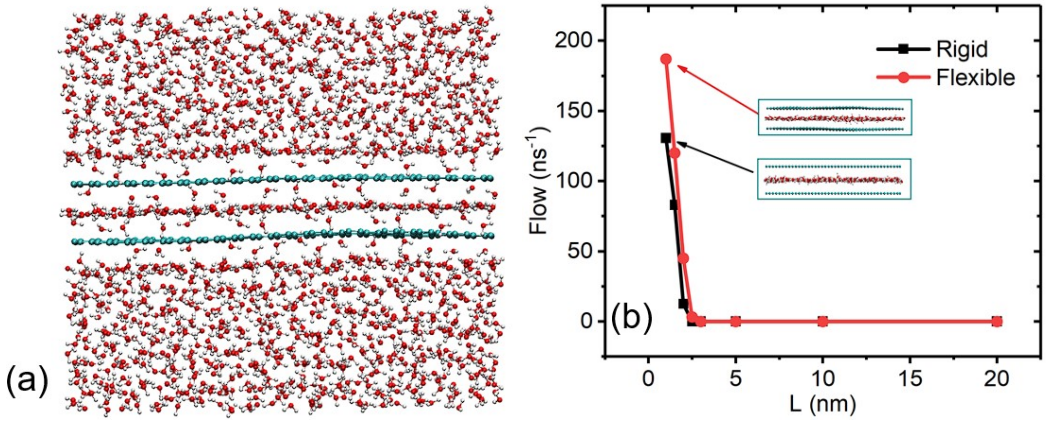

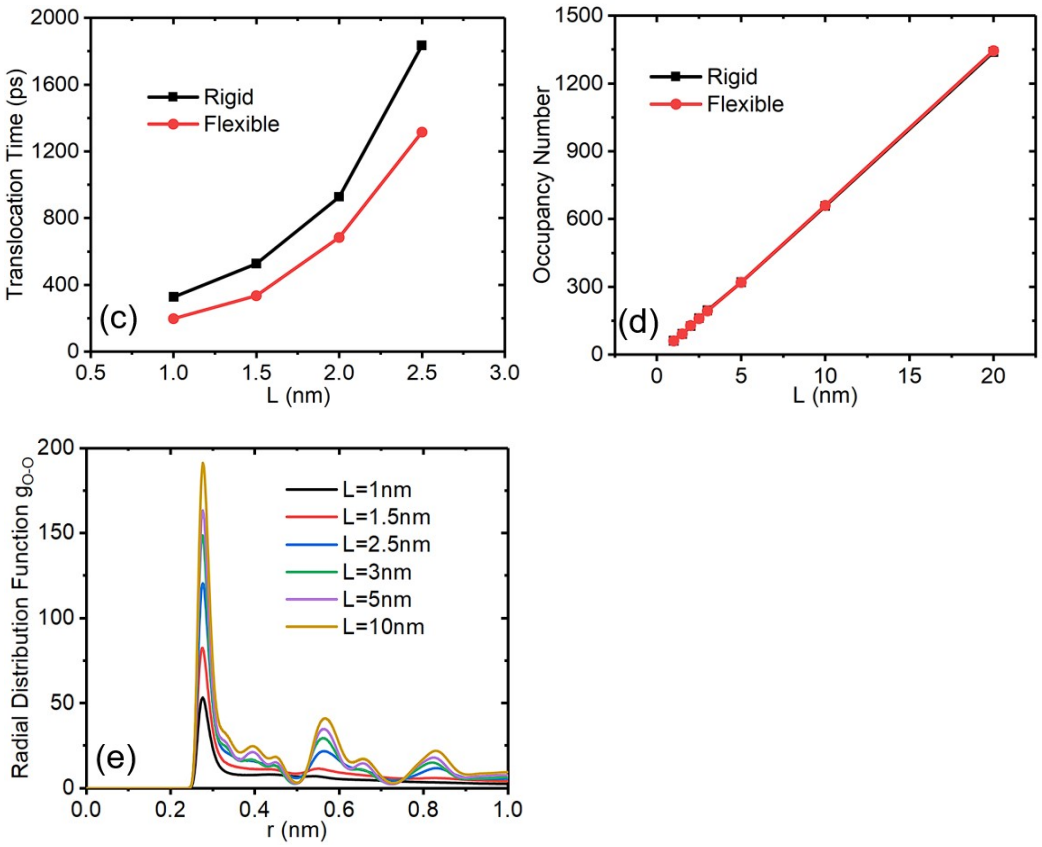

Figure S5. (a) Snapshot of the flexible graphene channel (release carbon atoms) without reservoirs. (b) Water flow, (c) translocation time and (d) occupancy umber as a function of the channel length. (e) Radial distribution functions of the confined water for the flexible graphene channel.

References

[S1] Baran, Ł.; Rżysko, W.; MacDowell, L. G. Self-Diffusion and Shear Viscosity for the TIP4P/Ice Water Model. J. Chem. Phys. 2023, 158, 064503.

[S2] Abascal, J. L. F.; Vega, C. A General Purpose Model for the Condensed Phases of Water: TIP4P/2005. J. Chem. Phys. 2005, 123, 234505.